Marked Wavelength Dependence in Photolyses of Dithiophosphate Complexes of the $[Mo^{V}_2O_3]^{4+}$ Core through a Photoactive Intermediate Accessed by a Secondary Thermal Equilibrium

Robert L. Thompson, Steven J. Geib, and N. John Cooper*

Department of Chemistry, University of Pittsburgh, Pittsburgh, Pennsylvania 15260

Received June 25, 1993®

Beer's law plots for the oxo-bridged d^1–d^1 dimers $[Mo_2O_3\{S_2P(OR)_2\}_4]$ (R = Et, **3**; R = Ph, **4**; R = Me, **5**) exhibit positive deviations from linearity, suggestive of dissociative equilibria. In the case of **3** it has been established by ^{31}P NMR that this is a consequence of the disproportionation equilibrium between **3** and its d^2 and d^0 disproportionation products $[MoO\{S_2P(OEt)_2\}_2]$ (**6**) and $[MoO_2\{S_2P(OEt)_2\}_2]$ (**7**), both of which have been independently prepared. ^{31}P NMR spectroscopy has been used to measure the dissociation constants, K_{diss}, for **3**, **4**, and **5** at various temperatures, and hence to determine ΔG_{298}, ΔH and ΔS values of 4.43 ± 0.05 kcal mol^{-1}, 12.1 ± 1.0 kcal mol^{-1}, and 25.6 ± 4.2 cal mol^{-1} K^{-1} for **3**; 4.08 ± 0.06 kcal mol^{-1}, 11.2 ± 1.3 kcal mol^{-1}, and 23.8 ± 4.2 cal mol^{-1} K^{-1} for **4**; and 3.68 ± 0.06 kcal mol^{-1}, 12.6 ± 1.0 kcal mol^{-1}, and 30.0 ± 4.5 cal mol^{-1} K^{-1} for **5**. A single-crystal diffraction study has established that **5** (monoclinic space group $P2_1/c$; with a = 8.235(3) Å, b = 16.544(5) Å, c = 11.444(5) Å, β = 103.79(2)°, Z = 2, and R = 4.7%) has a typical $[Mo^{V}_2O_3]^{4+}$ core with a linear bridging oxo group with an anti orientation for the terminal oxo groups. Solutions of **3**, **4**, and **5** are irreversibly bleached by UV light (<400 nm), but are unaffected by visible light (>400 nm) despite the presence of intense absorptions at 500 nm (ϵ_{500} = 11 800, 27 200, and 16 600 L mol^{-1} cm^{-1} respectively for **3**, **4**, and **5**). Disappearance quantum yields for photolysis of **3**, **4**, and **5** at various irradiation wavelengths are modest in the UV ($\Phi = 10^{-3}$–10^{-2}) but negligible at 510 nm ($\Phi_{510} < 10^{-4}$), giving rise to Φ_{310}:Φ_{510} ratios of >150, >180, and >60 respectively for **3**, **4**, and **5**. It is proposed that this marked wavelength dependence arises because the d^1–d^1 dimers are not themselves photoactive, but are destroyed through photolysis of the d^0 disproportionation products $[MoO_2\{S_2P(OR)_2\}_2]$ as confirmed for the case of **3** by independent determination of the disappearance quantum yield for **7** as 0.12 at 310 nm.

Introduction

We recently suggested that the photochromic behavior of the d^1–d^1 dithiocarbamate oxo-bridged dimers $[M^{V}_2O_3\{S_2CN(CH_2Ph)_2\}_4]$ (M = Mo or W) might have useful technical applications,[1] and we have been particularly interested in the possibility that the photochromism of these or related molecules containing the $[M^{V}_2O_3]^{4+}$ chromophore might provide the basis for photoactive materials which could be used in optical memory systems. The attractions of these systems include the dramatic change in optical density following photodisproportionation of the $[M^{V}_2O_3\{S_2CN(CH_3Ph)_2\}_4]$ dimers as a consequence of loss of the intense purple color characteristic of the $[M^{V}_2O_3]^{4+}$ chromophore (M = Mo, **1**, λ_{max} = 519 nm, ϵ = 19 000 M^{-1} cm^{-1}; M = W, **2**, λ_{max} = 517 nm, ϵ = 15 000 M^{-1} cm^{-1}) and the absence of strong visible absorptions in spectra of the d^0 and d^2 disproportionation products $[MO_2\{S_2CN(CH_2Ph)_2\}_2]$ and $[MO\{S_2CN(CH_2Ph)_2\}_2]$.

Any practical optical memory substrate would, however, have to fulfill many other technical criteria,[2] one of the most challenging of which is that the photochromism would have to exhibit marked wavelength dependence if there is to be a wavelength at which it is to be read many times without degradation. While exploring the photochemistry of other members of the large class of oxo-bridged dimers containing the $[Mo^{V}_2O_3]^{4+}$ core we have now discovered that the photochemistry of the dithiophosphate dimers $[Mo^{V}_2O_3\{S_2P(OR)_2\}_4]$ (**3**, R = Et; **4**, R = Ph; **5**, R = Me) offers a potential approach to the solution of this problem—unlike the dithiocarbamate dimers these dimers do not photodisproportionate when irradiated in the visible, but instead undergo a photolysis reaction which exhibits marked wavelength dependence in the *effective* disappearance quantum yields. This arises because the photoactivate species are actually the Mo^{VI} monomers $[Mo^{VI}O_2\{S_2P(OR)_2\}_2]$, accessible from **3**, **4**, and **5** through the thermal disproportionation equilibria shown in Scheme I.

Scheme I

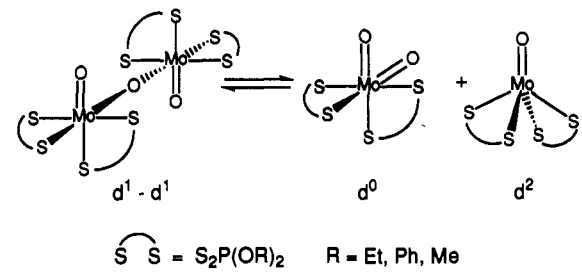

Experimental Section

General Data. All manipulations were carried out under a dry, oxygen free atmosphere except when specified otherwise. Aprotic solvents were freshly distilled under nitrogen from appropriate drying agents as follows: potassium metal for toluene and hexane; CaH_2 for CH_2Cl_2 and CH_3CN. Pentane was stirred over 5% HNO_3/H_2SO_4, neutralized with K_2CO_3, and distilled from CaH_2 before use. Anhydrous MeOH was purged with dry N_2 before use. CD_2Cl_2 (99.9 atom %, MSD) and $CDCl_3$ (99.8 atom %, MSD) were passed through basic activity I Al_2O_3 and purged with dry N_2 before use. Toluene-d_8 (99.6% and C_6D_6 (99.6%) were used as received from MSD. Pyridine *N*-oxide was dried in an Abderhalden drying pistol using crushed $CaCl_2$ under refluxing toluene. Aberchrome 540 was used as received.

Microanalyses were performed by Atlantic Microlabs, Inc., Norcross, GA. ^{31}P NMR spectra were recorded on a Bruker AM500 with 80% H_3PO_4 in H_2O as an external standard. Temperatures within the NMR probe for the ^{31}P NMR studies were controlled by a Bruker variable-temperature unit, which was calibrated against boiling and freezing distilled H_2O and is accurate to within 0.2 K. Samples were allowed to equilibrate thermally at each temperature for at least 10 min before

* Abstract published in *Advance ACS Abstracts*, September 15, 1993.

(1) Lee, S.; Staley, D. L.; Rheingold, A. L.; Cooper, N. J. *Inorg. Chem.* **1990**, *29*, 4391.

(2) (a) *Photochromism—Molecules and Systems*; Dürr, H., Bouas-Laurent, H., Eds.; Elsevier: Amsterdam, 1990. (b) Emmelius, M.; Pawlowski, G.; Vollman, H. W. *Angew. Chem., Int. Ed. Engl.* **1989**, *28*, 1445.

0020-1669/93/1332-6076$04.00/0

spectra were recorded. $HS_2P(OPh)_2$ was prepared from P_2S_5 and molten phenol according to the literature method.[3] $[MoO_2(acac)_2]$ was prepared from $(NH_4)_6Mo_7O_{24}\cdot 4H_2O$ and 2,5-pentanedione according to an adaptation of the literature method.[4] $[Mo_2O_3\{S_2P(OEt)_2\}_4]$ (3) was prepared in MeOH from $[MoO_2(acac)_2]$ and $HS_2P(OEt)_2$ according to an adaptation of the method described by Chen et al.[4] $[MoO\{S_2P(OEt)_2\}_2]$ (6) was prepared according to an adaptation of the method described by Jowitt and Mitchell from $[Mo_2O_3\{S_2P(OEt)_2\}_4]$ and Zn dust in refluxing CH_2Cl_2.[5] The $[MoO\{S_2P(OEt)_2\}_2]$ obtained in this way is not contaminated with PPh_3 or $OPPh_3$, as is the case with the method of Chen et al.[4]

$[Mo_2O_3\{S_2P(OPh)_2\}_4]$ (4). A mixture of $[MoO_2(acac)_2]$ (2.00 g, 6.14 mmol), $HS_2P(OPh)_2$ and PhOH (60 g, ≈640 mmol) were heated in an oil bath to 60 °C and stirred for 1.5 h. The dark maroon PhOH melt was poured into 500 mL of H_2O. The dark precipitate of the product was filtered, washed with hexanes (3 × 30 mL), and vacuum dried to give $[Mo_2O_3\{S_2P(OPh)_2\}_4]$ (2.35 g, 1.72 mmol = 28%). The ^1H and ^{31}P NMR spectra of the product matched those reported in the literature.[6,7] ^1H NMR (C_6D_6, 300 MHz): δ 6.97–6.75 (br m, 8 OC_6H_5). ^{31}P NMR (toluene-d_8, 202 MHz): δ 130.4 (s, Mo^{IV}), 100.5 (br s, Mo^V), 93.5 (s, Mo^{VI}). Anal. Calcd for $C_{48}H_{40}Mo_2O_{11}P_4S_8$: C, 42.23; H, 2.95. Found: C, 42.17; H, 3.02.

$[Mo_2O_3\{S_2P(OMe)_2\}_4]$ (5). Addition of $HS_2P(OPh)_2$ (22.2 g, 78.7 mmol) to a suspension of $[MoO_2(acac)_2]$ (8.00 g, 24.5 mmol) in 200 mL of MeOH at room temperature resulted in the precipitation of a dark maroon solid. After 4 h the stirred mixture was cooled to 0 °C and allowed to settle. The maroon precipitate was isolated by decantation, washed with MeOH (2 × 50 mL) and then recrystallized from a 3:1 mixture of pentane and toluene. After 3 days a dark maroon solid formed, which was decanted and vacuum-dried to give $[Mo_2O_3\{S_2P(OMe)_2\}_4]$ (4.86 g, 5.56 mmol = 45% yield). The ^1H and ^{31}P NMR spectra of the product matched those reported in the literature.[7] ^1H NMR ($CDCl_3$, 300 MHz): δ 3.89, br d, J_{P-H} = 15.2 Hz, 24 H, OCH_3). ^{31}P NMR (toluene-d_8, 202 MHz): δ 139.9 (s, Mo^{IV}), 102.7 (br s, Mo^V), 95.1 (s, Mo^{VI}). Anal. Calcd for $C_8H_{24}Mo_2O_{11}P_4S_8$: C, 11.06; H, 2.79. Found: C, 11.12; H, 2.73.

$[MoO_2\{S_2P(OEt)_2\}_2]$ (7). Addition of pyridine *N*-oxide (0.51 g, 5.36 mmol) to a maroon solution of $[Mo_2O_3\{S_2P(OEt)_2\}_4]$ (4.00 g, 4.08 mmol) in toluene at room temperature resulted in a color change to deep yellow. The mixture was stirred for 1 h at room temperature and was then concentrated to ca. 10 mL. Pentane (50 mL) was added and the mixture placed at −80 °C for 3 days to give golden-brown plates of $[MoO_2\{S_2P(OEt)_2\}_2]$ (1.67 g, 3.35 mmol = 41% yield). ^1H NMR ($CDCl_3$, 300 MHz): δ 4.23 (br q, 8 H, $^3J_{HH}$ = 7.09 Hz, 4 CH_2), 1.38 (t, 12 H, $^3J_{HH}$ = 7.09 Hz, 4 CH_3). Anal. Calcd for $C_8H_{12}MoO_6P_2S_4$: C, 19.28; H, 4.05. Found: C, 19.34; H, 4.09.

X-ray Diffraction Study of $[Mo_2O_3\{S_2P(OMe)_2\}_4]$ (5). A blue-green crystal of **5** was coated in epoxy cement and attached to a fine glass fiber. The crystal of **5** was uniquely assignable to monoclinic space group $P2_1/c$ on the basis of photographic evidence and systematic absences. Unit cell dimensions were derived from the least squares fit of the angular settings of 25 reflections with 18° ≤ 2θ ≤ 25°. Diffraction data were collected as summarized in Table I. A profile fitting procedure was applied to all data to improve the precision of the measurement of weak reflections. A semiempirical absorption correlation (XEMP) was applied to the diffraction data. Diffraction data were corrected for extinction effects.

The structure was solved by means of the direct methods routine TREF, which located the Mo, P, and S atoms. The remaining non-hydrogen atoms were located from subsequent Fourier syntheses and refined anisotropically. Hydrogen atoms were placed in idealized calculated positions (d(C–H) = 0.96 Å). The asymmetric unit consits of a half molecule of **5**. The molecule resides on a center of symmetry site with O(1) located at (0, $^1/_2$, 0). The highest peak in the final difference Fourier synthesis corresponded to 1.28 e Å^{-3} and was close to the metal center. Inspection of F_o vs F_c values and trends based on sin θ, Miller indices, and parity groups failed to reveal any systematic errors in the X-ray data. Atomic coordinates are listed in Table II, selected bond lengths in Table III, and selected bond angles in Table IV. All computer programs used in the collection, solution, and refinement of crystal data are contained in the Siemens program package SHELXTL PLUS (VMS version 4.2).

Quantum Yield Determinations. Quantum yields were determined in a manner similar to that reported by Wegner and Adamson for the measurement of the photoaquation of Reinecke's salt.[8] An air-cooled 200 Watt Oriel mercury–xenon arclamp was used as the light source, and

Table I. Summary of Crystal Data, Data Collection, and Refinement Parameters for $[Mo_2O_3\{S_2P(OMe)_2\}_4]$ (5)

Crystal Data	
formula	$C_8H_{24}O_{11}P_4S_8Mo_2$
cryst syst	monoclinic
space group	$P2_1/c$
a, Å	8.235(3)
b, Å	16.544(5)
c, Å	11.444(5)
β, deg	103.79(2)
V, Å^3	1514(1)
Z	2
ρ (calcd), g cm^{-3}	1.905

Data Collection	
μ, cm^{-1}	16.33
temp, °C	24
cryst dimens, mm	0.16 × 0.23 × 0.25
radiation	Mo Kα (λ = 0.710 73 Å), graphite-monochromated
diffractometer	Siemens R3m/V
scan speed, deg min^{-1}	variable, 5–20
2θ scan range, deg	4 < 2θ < 48
scan technique	ω
data collcd	$+h,+k,\pm l$
weighting factor, g	0.001
no. of unique data	2366 (2908 read)
no. of unique data with $F_o > 6(F_o)$	1527
std rflns	3/197

Agreement Factors			
R, %	4.70	max peak, e Å^{-3}	1.28
R_w, %	5.56	data:param	10:1
GOF	1.30	D/σ	0.001

Table II. Fractional Atomic Coordinates (×10^4) and Equivalent Isotropic Displacement Coefficients[a] (Å × 10^3) for $[Mo_2O_3\{S_2P(OMe)_2\}_4]$ (5)

	x	y	z	U(eq)
Mo	1958(1)	4921(1)	1204(1)	38(1)
S(1)	1544(4)	3470(1)	1681(2)	64(1)
S(2)	−220(3)	4952(1)	2744(2)	52(1)
S(3)	1954(3)	6392(1)	1466(2)	48(1)
S(4)	4177(3)	5075(1)	3169(2)	52(1)
P(1)	−106(3)	3773(1)	2643(2)	52(1)
P(2)	3925(3)	6256(1)	2887(2)	47(1)
O(1)	0	5000	0	43(3)
O(2)	3355(8)	4702(4)	415(6)	60(2)
O(3)	357(8)	3333(4)	3909(6)	68(3)
O(4)	−1778(10)	3343(4)	2112(10)	116(5)
O(5)	5525(8)	6699(4)	2709(6)	64(3)
O(6)	3770(8)	6746(3)	4033(5)	60(2)
C(1)	1834(15)	3497(7)	4771(9)	87(5)
C(2)	−3304(12)	3653(6)	1646(10)	71(4)
C(3)	6242(13)	6493(7)	1710(9)	78(5)
C(4)	2417(14)	6581(6)	4594(10)	80(5)

[a] Equivalent isotropic U defined as one-third of the trace of the orthogonalized U_{ij} tensor.

Table III. Bond Lengths (Å) within $[Mo_2O_3\{S_2P(OMe)_2\}_4]$ (5)

Mo–S(1)	2.504(3)	Mo–S(2)	2.799(3)
Mo–S(3)	2.453(2)	Mo–S(4)	2.549(2)
Mo–O(1)	1.859(1)	Mo–O(2)	1.663(7)
S(1)–P(1)	2.006(4)	S(2)–P(1)	1.956(3)
S(3)–P(2)	2.018(3)	S(4)–P(2)	1.983(3)
P(1)–O(3)	1.584(7)	P(1)–O(4)	1.541(8)
P(2)–O(5)	1.562(7)	P(2)–O(6)	1.573(7)
O(3)–C(1)	1.398(12)	O(4)–C(2)	1.344(12)
O(5)–C(3)	1.447(14)	O(6)–C(4)	1.439(14)

(3) Lefferts, J.; Molloy, K. C.; Zuckerman, J. J.; Haiduc, I.; Guta, C.; Ruse, C. *Inorg. Chem.* **1980**, *19*, 1662.
(4) Chen, G. J. J.; McDonald, J. W.; Newton, W. E. *Inorg. Chem.* **1976**, *15*, 2612.
(5) Jowitt, R. N.; Mitchell, P. C. H. *J. Chem. Soc. A* **1969**, 2632.
(6) Jowitt, R. N.; Mitchell, P. C. H. *J. Chem. Soc. A* **1970**, 1702.
(7) Ratnani, R.; Srivistava, G.; Mehrotra, R. C. *Inorg. Chim. Acta* **1989**, *161*, 253.

Table IV. Bond Angles (deg) Within $[Mo_2O_3\{S_2P(OMe)_2\}_4]$ (**5**)

S(1)–Mo–S(2)	74.9(1)	S(1)–Mo–S(3)	157.1(1)
S(2)–Mo–S(3)	83.4(1)	S(1)–Mo–S(4)	90.6(1)
S(2)–Mo–S(4)	82.8(1)	S(3)–Mo–S(4)	79.3(1)
S(1)–Mo–O(1)	95.1(1)	S(2)–Mo–O(1)	83.8(1)
S(3)–Mo–O(1)	89.7(1)	S(4)–Mo–O(1)	163.6(1)
S(1)–Mo–O(2)	93.2(2)	S(2)–Mo–O(2)	167.4(2)
S(3)–Mo–O(2)	107.7(2)	S(4)–Mo–O(2)	93.3(2)
O(1)–Mo–O(2)	101.7(2)	Mo–S(1)–P(1)	91.4(1)
Mo–S(2)–P(1)	84.1(1)	Mo–S(3)–P(2)	87.9(1)
Mo–S(4)–P(2)	86.0(1)	S(1)–P(1)–S(2)	109.3(2)
S(1)–P(1)–O(3)	109.9(3)	S(2)–P(1)–O(3)	114.2(3)
S(1)–P(1)–O(4)	109.0(4)	S(2)–P(1)–O(4)	115.6(3)
O(3)–P(1)–O(4)	98.4(5)	S(3)–P(2)–S(4)	105.9(1)
S(3)–P(2)–O(5)	112.6(3)	S(4)–P(2)–O(5)	115.1(3)
S(3)–P(2)–O(6)	113.9(3)	S(4)–P(2)–O(6)	113.5(3)
O(5)–P(2)–O(6)	96.1(4)	Mo–O(1)–Moa	180
P(1)–O(3)–C(1)	122.3(7)	P(1)–O(4)–C(2)	130.0(6)
P(2)–O(5)–C(3)	120.6(6)	P(2)–O(6)–C(4)	120.0(6)

the light was collimated to give a beam of about 1 cm^2 in area which was passed through a water filter and a variable iris before monochromatization by appropriate interference filters (Oriel; 310, 334, 365, or 510 nm). The collimated, monochromatic light beam was passed through sample cells in a brass thermostated cell holder, the temperature of which was controlled to ±0.2 °C using a circulating bath of 50% ethylene glycol/H_2O. The temperature within the cell holder was monitored by a Fluke K-type thermocouple. Absorbances of irradiated samples were measured by rapidly transferring the cells to an IBM 9430 spectrometer fitted with a second thermostated cell holder, which was connected to the same circulating bath as the irradiation cell holder through glass T-joints and insulated rubber tubing.

The lamp output was determined immediately before each quantum yield measurement by means of an Aberchrome 540 chemical actinometer. This consisted of a toluene solution of the heterocyclic fulgide, (*E*)-α-(2,5-dimethyl-3-furylethylidene)(isopropylidene)succinic anhydride[9] of known concentration and volume sealed inside a 1.00-cm quartz cell under vacuum. Aberchrome 540 undergoes a highly reversible conrotatory ring-closure reaction to give deep red 7,7a-dihydro-2,4,7,7,7a-pentamethylbenzo[*b*]furan-5,6-dicarboxylic anhydride,[10] and the known quantum yields for the forward and reverse reactions were used to measure intensities in the 310-370- and 436-545-nm ranges, respectively, from plots of the absorbance increase or decrease at 494 nm versus time and application of the relation $I = (V/\Phi_A\epsilon_A l)(\Delta A/t)$ where I is the intensity in einstein s^{-1}, V is the solution volume (3.00×10^{-3} L), Φ_A is the forward or reverse quantum yield for Aberchrome 540 photolysis (0.20 and 0.06), ϵ_A is the extinction coefficient for Aberchrome 540 at 494 nm (8,200 L mol^{-1} cm^{-1}), l is the cell length (1.00 cm), and $\Delta A/t$ is the slope from the absorbance versus time plot (s^{-1}).[10]

After the lamp intensity measurement, sample solutions of known volume were allowed to equilibrate thermally in the dark for at least 10 min and were then irradiated for periods such that absorbance at 500 nm decayed no more than 10–15% from the absorbance at $t = t_0$. Concentrations of sample solutions were chosen such that the absorbance at the irradiation wavelength was >1.7 absorbance units (>98% incident intensity absorption) and that the absorbance at the measuring wavelength (500 nm) was no larger than 2.2–2.3 absorbance units to ensure readibility. Quantum yields Φ were determined from the slope of plots of ΔA at 500 nm versus t by means of the same relationship as that above. Each quantum yield reported at a particular wavelength is the average of three values obtained in independent runs.

Results and Discussion

Our study of the photolysis of dithiophosphate complexes of the $[Mo^{V}_2O_3]^{4+}$ core began as an extension of our observation that the dithiocarbamate complexes $[M^{V}_2O_3\{S_2CN(CH_2Ph)_2\}_4]$ (M = Mo, **1**; W, **2**) photodisproportionate to give the d^0 and d^2 monomers $[MO_2\{S_2CN(CH_2Ph)_2\}_2]$ and $[MO\{S_2CN(CH_2Ph)_2\}_2]$.[1] Our initial study established that this photodisproportionation resulted in marked photochromic behavior by solutions of **1** and **2**, but quantitative studies were rendered experimentally difficult by the speed of the thermal recombination of the d^0 and d^2 disproportionation products. The d^1–d^1 dimers **1** and **2** are, however, members of a large class of d^1–d^1 oxo-bridged dimers (most commonly of Mo(V)) containing $[M_2O_3]^{4+}$ cores,[11] and we reasoned that other members of this class might prove more amenable to quantum yield and other photochemical studies if, for example, recombination of d^0 and d^2 monomers were slower or if it proved feasible to trap one of the monomers.

We chose dithiophosphate analogs of **1** and **2** for further study because the literature indicated that several examples of such complexes were readily accessible synthetically ($[Mo^{V}_2O_3\{S_2P(OEt)_2\}_4]$ (**3**)[4,6,7] and $[Mo^{V}_2O_3\{S_2P(OPh)_2\}_4]$ (**4**)[6,7]), and because it also seemed probable that the ligands in **3** and **4** were sufficiently distinct electronically that at least one of the complexes would give rise to a pair of disproportionation products in which both the Mo^{VI} and the Mo^{IV} component would be stable, as is the case with **1** and **2**, so that the equilibrium would be straightforward to study.

Syntheses of Dialkyl Dithiophosphate Complexes. The literature on $[Mo_2O_3\{S_2P(OEt)_2\}_4]$ (**3**) provides a reliable, high yield synthesis of **3** from $[MoO_2(acac)_2]$,[4] but we were frustrated in our initial attempts to prepare $[Mo_2O_3\{S_2P(OPh)_2\}_4]$ (**4**) by an extension of the route to **3** because of a rapid alkoxide exchange reaction between $HS_2P(OPh)_2$ and the MeOH solvent[12] which resulted in the isolation of $[Mo_2O_3\{S_2P(OMe)_2\}_4]$ (**5**) rather than **4**, a result in sharp contrast with a literature report that **4** can be prepared in this way.[7] The facility of this exchange was at first surprising, but is reasonable. The facility of the exchange was independently established by an experiment in which a CD_2Cl_2 solution of $HS_2P(OPh)_2$ was treated with 1 equiv of MeOH at room temperature and the ^1H NMR spectrum of the mixture was recorded every 10 min. The initially observed multiplet at δ 7.47–7.31 assigned to $HS_2P(OPh)_2$ was gradually replaced by multiplets at 7.21 and 6.83, which correspond to the resonances of phenol, and the CH_3OH resonance at δ 3.42 was replaced by a doublet at δ 3.81 (J_{P-H} = 15.4 Hz) assigned to the methoxy protons of $HS_2P(OMe)_2$. The exchange generates no other stray NMR signals, suggesting that the reaction is clean. The alkoxide exchange reaction was complete after 1 h.

Attempts to prepare **4** from $[MoO_2(acac)_4]$ in the bulky alcohol ^{i}PrOH were also unsuccessful, since an exchange reaction was again observed between the $HS_2P(OPh)_2$ reagent and the ^{i}PrOH solvent. The reaction was, however, more complex than in the MeOH case, and the ^1H NMR spectrum in C_6D_6 of the product from this reaction displayed a broad lump between δ 4.9 and 5.3 assigned to isopropoxy methine protons and numerous doublets between δ 1.24 and 0.95 assigned to isopropoxy methyl protons. This reaction was clearly complex and was not pursued, although the complex $[Mo_2O_3\{S_2P(O^iPr)_2\}_4]$ has been reported.[13]

The preparation of complex **4** was finally achieved by eliminating the possibility of exchange through the use of molten PhOH as the solvent. A mixture of $[MoO_2(acac)_2]$ and $HS_2P(OPh)_2$ slowly turned maroon in molten PhOH at 60 °C. After 1.5 h, the PhOH melt was poured into H_2O to precipitate the product in a reproducible yield of ca. 30%. The ^1H NMR and ^{31}P NMR spectra recorded for **3** prepared in this way conformed to those previously reported.[6,7]

The exchange reaction between MeOH and $HS_2P(OPh)_2$ provided a convenient preparation of $[Mo_2O_3\{S_2P(OMe)_2\}_4]$ (**5**) without the need to prepare the free $HS_2P(OMe)_2$ ligand since the available supply of $HS_2P(OPh)_2$ could be used as the ligand

(8) Wegner, E. E.; Adamson, A. W. *J. Am. Chem. Soc.* **1966**, *88*, 394.
(9) Davey, P. J.; Heller, H. G.; Strydon, P. J.; Whittall, J. *J. Chem. Soc., Perkin Trans. 2* **1981**, 202.
(10) Heller, H. G.; Langan, J. R. *J. Chem. Soc. Perkin Trans. 2* **1981**, 341.
(11) (a) Steifel, E. I. *Prog. Inorg. Chem.* **1977**, *22*, 1. (b) Holm, R. H. *Chem. Rev.* **1987**, *87*, 1401. (c) Holm, R. H. *Coord. Chem. Rev.* **1990**, *100*, 183. (d) Garner, C. D.; Charnock, J. M. In *Comprehensive Coordination Chemistry*; Wilkinson, G., Gillard, R. D., McCleverty, J., Eds; Pergamon: Oxford, England, 1987; Vol. 3, Part 36.4.
(12) Closely related exchanges have been reported; see e.g.: Feringa, B. L. *J. Chem. Soc., Chem. Commun.* **1987**, 695.
(13) Aliev, Z. G.; Atovmyan, L. O.; Tkachev, V. V. *Zh. Strukt. Khim.* **1975**, *16*, 646.

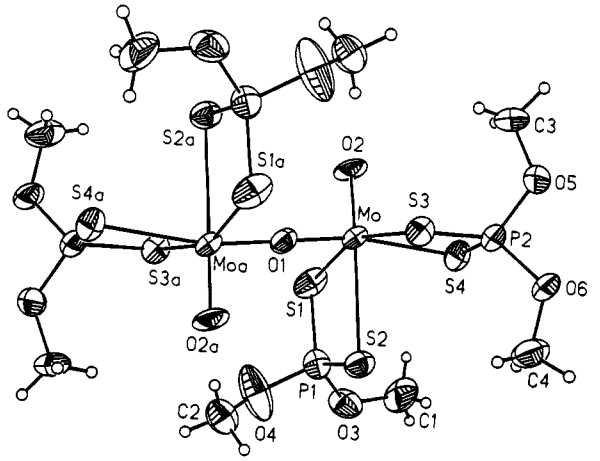

Figure 1. Molecular structure of $[Mo_2O_3\{S_2P(OCH_3)_2\}_4]$ (**5**) (40% probability ellipsoids). Atoms with an "a" subscript are symmetry generated by inversion through the bridging oxygen atom.

source. A mixture of $[MoO_2(acac)_2]$ and $HS_2P(OPh)_2$ was simply allowed to stir in MeOH for 4 h to give a maroon precipitate of **5**. This procedure led to a good recrystallized yield of samples of **5**.

The anticipated Mo(IV) product of disproportionation of **3** ($[MoO\{S_2P(OEt)_2\}_2]$ (**6**)) had been previously reported and could be prepared by the literature method,[5] but the Mo(VI)–dioxo complex has not previously been reported. Work by Mitchell and Scarle[14] reporting the oxidation of $[MoO(S_2CNEt_2)_2]$ using pyridine *N*-oxide suggested that $[MoO_2\{S_2P(OEt)_2\}_2]$ (**7**) might be accessible via oxidation of **3** with pyridine *N*-oxide, and we readily established that solutions of **3** quickly changed color from deep purple to yellow upon addition of an equivalent of pyridine *N*-oxide. Isolation of complex **7** was not straightforward because evaporation of these solutions under vacuum caused the color to revert to deep maroon. The Mo(VI) product could, however, be isolated by addition of pentane to the concentrated solution to precipitate the product at −80 °C. This procedure provided analytically pure **7** in moderate yield. With **7** in hand, we now had independent access to all three members of the disproportionation equilibrium between **3**, **6**, and **7**.

Solid-State Structure of $[Mo_2O_3\{S_2P(OMe)_2\}_4]$ (5). The ethyl complex **3**[15] and the isopropyl complex $[Mo_2O_3\{S_2P(O^iPr)_2\}_4]$[13] have been characterized crystallographically, but no structural characterization has been reported for **5**. Since **5** is the archetypal dithiophosphate complex of the $[Mo^V_2O_3]^{4+}$ core (and the available diffraction study of the homologous complex is of limited precision), it was appropriate to determine the solid of the structure of **5**. We particularly wanted to determine whether the terminal oxo bridges in **5** adopt a syn or an anti conformation with respect to the linear oxo bridge, since, although we anticipated an anti conformation analogous to that found for **3**, we recently demonstrated that dithiocarbamate and xanthate complexes of the $[Mo^V_2O_3]^{4+}$ core exist as mixtures of syn and anti isomers in solution,[16] and hence that there is only a small free energy difference between these isomers in some systems closely related to **5**. The single crystal X-ray diffraction study described in the Experimental Section readily allowed us to establish that the terminal oxo atoms of **5** adopt an anti conformation in the solid state (Figure 1) analogous to those adopted by **3** and $[Mo_2O_3\{S_2P(O^iPr)_2\}_4]$,[13] with a perfectly linear oxo bridge between the Mo centers as a consequence of the location of the bridging oxygen atom at the crystallographic center of inversion. The Mo atoms

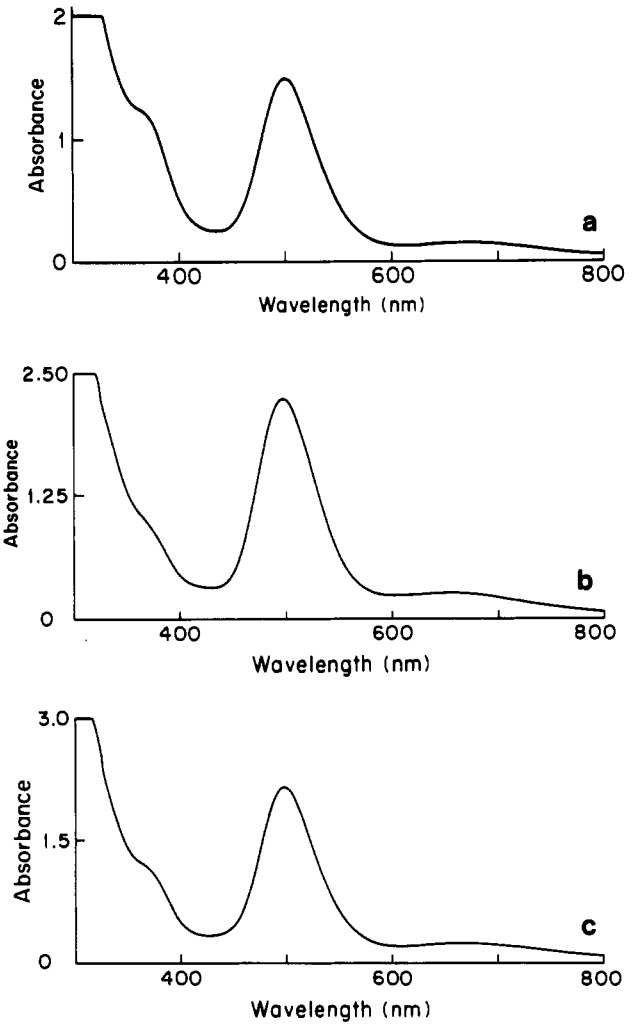

Figure 2. Electronic spectra in toluene for solutions of (a) $[Mo_2O_3\{S_2P(OEt)_2\}_4]$ (1.28×10^{-4} mol L^{-1}), (b) $[Mo_2O_3\{S_2P(OPh)_2\}_4]$ (8.27×10^{-5} mol L^{-1}), and (c) $[Mo_2O_3\{S_2P(OMe)_2\}_4]$ (1.46×10^{-4} mol L^{-1}.

have distorted octahedral coordination geometries with Mo–O_b bond lengths of 1.859(1) Å and Mo–O_t bond lengths of 1.663(7) Å, reflecting the partial double bond character of the bridging oxo bonds and the full double bond character of the terminal oxo bonds. The Mo–S bond lengths vary, with the Mo–S bond trans to the Mo–O_t bond being the longest at 2.799(3) Å while the remaining Mo–S bonds range from 2.453(2) to 2.549(2) Å.

Disproportionation Equilibria in Solutions of 3, 4, and 5 and Their Effects on Electronic and ^{31}P NMR Spectra. Initial electronic spectra of **3**, **4**, and **5** in toluene were straightforward (Figure 2) and were dominated by strong absorptions ($\epsilon > 10^4$) in the visible at 500 nm for all three complexes. Strong absorptions at ca 500 nm are characteristic of the $[M^V_2O_3]^{4+}$ functional group when coordinated to bischelating sulfur ligands[17] like dithiocarbamates,[6,18] xanthates,[19] or dithiophosphates,[6,7] and we initially assumed that the strength of the absorptions implied that **3**, **4**, and **5** did exist as dimers in solution. Beer's law plots (Figure 3) readily established, however, that the situation was more complex, since all three complexes exhibited marked positive deviations suggestive of dissociative equilibria as shown in Scheme I.

To confirm that this disproportionation equilibrium was responsible for the Beer's law deviations it was necessary to

(14) Mitchell, P. C. H.; Scarle, R. D. *J. Chem. Soc., Dalton Trans.* **1975**, 2552.
(15) Knox, J. R.; Prout, C. K. *Acta Crystallogr., Sect. B* **1969**, *B25*, 2281.
(16) Thompson, R. L.; Lee, S.; Geib, S. J.; Cooper, N. J. *Inorg. Chem.*, preceding paper in this issue.
(17) (a) Lincoln, S.; Koch, S. A. *Inorg. Chem.* **1986**, *25*, 1594. (b) Craig, J. A.; Harlan, E. W.; Snyder, B. S.; Whitener, M. A.; Holm, R. H. *Inorg. Chem.* **1989**, *28*, 2082 and references therein.
(18) Moore, F. W.; Larson, M. L. *Inorg. Chem.* **1967**, *6*, 998.
(19) Newton, W. E.; Corbin, J. L.; McDonald, J. W. *J. Chem. Soc., Dalton Trans.* **1974**, 1044.

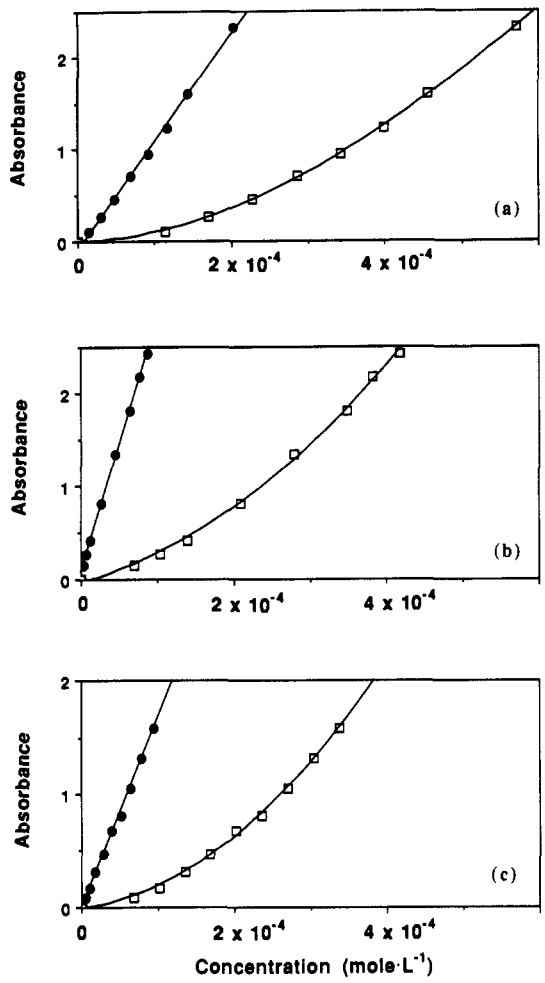

Figure 3. Beer's law plots for toluene solutions of (a) $[Mo_2O_3\{S_2P(OEt)_2\}_4]$ (**3**), (b) $[Mo_2O_3\{S_2P(OPh)_2\}_4]$ (**4**), and (c) $[Mo_2O_3\{S_2P(OMe)_2\}_4]$ (**5**). Figures show plots corrected (●) and uncorrected (□) for dissociation equilibria.

determine independently the equilibrium constants for the equilibria and use these values to correct the Beer's law data. The only previous determination of the dissociation constant for any of these complexes is from the study by Tanaka and co-workers, who used concentration–jump relaxation kinetics methods to determine $K_{diss} = 3.9 \times 10^{-3}$ M for **3** in 1,2-dichloroethane at 25 °C.[20] This approach is not, however, experimentally convenient, and we also needed to determine K_{diss} in a solvent less likely to be reactive under photochemical conditions. We therefore turned to ^{31}P NMR studies of **3**, **4**, and **5**, reasoning that the ligand resonances in the Mo(V) dimers were likely to be distinct from those of the disproportionation products.

^{31}P NMR spectra of **3** in toluene are straightforward (Figure 4) and contain a single broad resonance at δ 97.3 assigned to the Mo^V dimer flanked by narrower peaks at δ 136.5 and δ 89.3 assigned to the disproportionation products $[Mo^{IV}O\{S_2P(OEt)_2\}_2]$ (**6**) and $[Mo^{VI}O\{S_2P(OEt)_2\}_2]$ (**7**) respectively. These assignments were unambiguously confirmed by comparison with spectra of samples of **6** and **7** independently prepared as discussed above, and the equality in intensity of the signals from samples of **3** confirmed that they arose from **6** and **7** present as a consequence of in situ disproportionation of **3**.

The width of the peak assigned to **3** probably reflects fluxional behavior in this dimer. We have previously reported that the xanthate dimers $[Mo_2O_3(S_2COR)_4]$ (R = ^{i}Pr and Et) and the dithiocarbamate dimer $[Mo_2O_3\{S_2CN(CH_2Ph)_2\}_4]$ (**1**) all participate in intramolecular bridge/terminal oxo exchange reactions which are rapid on the NMR time scale and which exchange ligands with S trans to terminal oxo groups with ligands with S trans to the bridging oxo group.[16] The solid-state structure of $[Mo_2O_3\{S_2P(OEt)_2\}_4]$[15] indicates that **3** also contains two types of dithiophosphate ligands, those with one S trans to the bridging oxo group and those with one S trans to the terminal oxo group perpendicular to the Mo–O–Mo group. Since a single resonance is observed for the ^{31}P nuclei in **3**, these ligands must be equilibrated rapidly on the NMR time scale in solution, probably by a bridge/terminal oxo exchange similar to that proposed for the xanthate and dithiocarbamate complexes.[16]

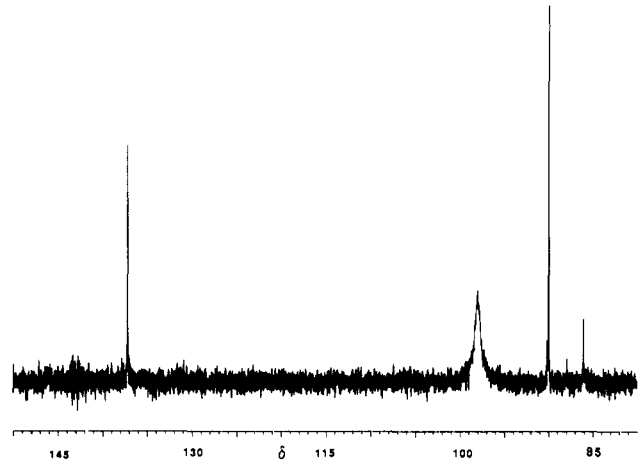

Figure 4. ^{31}P NMR spectrum of $[Mo_2O_3\{S_2P(OEt)_2\}_4]$ (**3**) in toluene at 27.0 °C.

Table V. Summary of ^{31}P NMR Data for Toluene-d_8 Solutions of Molecules **3–11**

complex	^{31}P chem shifts/δ
$[Mo^V_2O_3\{S_2P(OEt)_2\}_4]$ (**3**)	97.3
$[Mo^V_2O_3\{S_2P(OPh)_2\}_4]$ (**4**)	100.5
$[Mo^V_2O_3\{S_2P(OMe)_2\}_4]$ (**5**)	102.7
$[Mo^{IV}O\{S_2P(OEt)_2\}_2]$ (**6**)	136.5
$[Mo^{VI}O_2\{S_2P(OEt)_2\}_2]$ (**7**)	89.3
$[Mo^{IV}O\{S_2P(OPh)_2\}_2]$ (**8**)	130.4
$[Mo^{VI}O_2\{S_2P(OPh)_2\}_2]$ (**10**)	93.5
$[Mo^{IV}O\{S_2P(OMe)_2\}_2]$ (**9**)	139.9
$[Mo^{VI}O_2\{S_2P(OMe)_2\}_2]$ (**11**)	95.1

^{31}P spectra of **4** and **5** were similar to those of **3** and also contained signals assigned to the Mo(IV) and Mo(VI) disproportionation products $[Mo^{IV}O\{S_2P(OR)_2\}_2]$ (R = Ph, **8**; R = Me, **9**) and $[Mo^{VI}O_2\{S_2P(OR)_2\}_2]$ (R = Ph, **10**; R = Me, **11**). Assignments of these signals could be unambiguously made by analogy with the assignments for **6** and **7**, and complexes **9–11** were not prepared independently. ^{31}P NMR assignments for **3–11** are summarized in Table V.

^{31}P NMR spectra of **3**, **4**, and **5** were recorded at a variety of temperatures to obtain values for the dissociation constants at different temperatures. Integrations of the resonances from all three species present in each solution at each temperature were used to obtain the relative mole fractions of the corresponding Mo(IV), Mo(V), or Mo(VI) complexes. The integrations of the Mo(V) and Mo(VI) peaks sometimes overlapped slightly such that the integration of the Mo(VI) peak could not always be measured. In these instances, the integration of the Mo(IV) species was assumed to represent the mole fraction of both the Mo(IV) and Mo(VI) species; this assumption was borne out by the equality in size of these integrations when the Mo(VI) signal did not overlap. The mole fractions and the known initial concentration of **3** in the solution were then used to calculate the corresponding dissociation constants K_{diss} as presented in Table VI.

The precision of the NMR studies was confirmed by the use of the ^{31}P based dissociation constants to correct the Beer's law

(20) Tanaka, T.; Tanaka, K.; Matsuda, T.; Hashi, K. In *Molybdenum Chemistry of Biological Significance*; Newton, W. E.; Otsuka, K., Eds.; Plenum Press: New York, 1980; p 361.

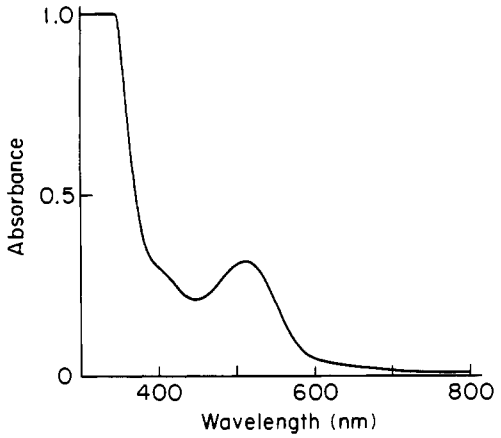

Figure 5. Electronic spectrum of $[MoO\{S_2P(OEt)_2\}_2]$ (**6**) in toluene.

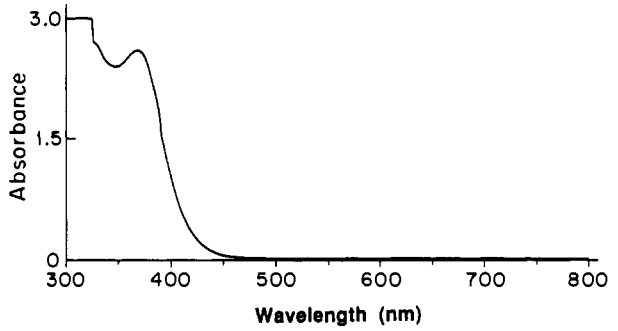

Figure 6. Electronic spectrum of $[MoO_2\{S_2P(OEt)_2\}_2]$ (**7**) in toluene.

Table VI. Equilibrium Constants and Thermodynamic Parameters for Disproportionation of $[Mo_2O_3\{S_2P(OR)_2\}_4]$ Complexes in Toluene

R	T, K	K_{diss}, M × 10^3	ΔG_{298}, kcal mol^{-1}	ΔH, kcal mol^{-1}	ΔS, cal mol^{-1} K^{-1}
Et (**3**)	280	0.17 ± 0.03			
	285	0.23 ± 0.04			
	290	0.31 ± 0.06			
	295	0.44 ± 0.08			
	300	0.56 ± 0.11	+4.43 ± 0.05	+12.1 ± 1.0	+25.6 ± 4.2
	305	0.84 ± 0.16			
	310	1.19 ± 0.22			
	315	1.70 ± 0.31			
	320	2.36 ± 0.44			
	325	3.31 ± 0.61			
Ph (**4**)	280	0.31 ± 0.07			
	290	0.58 ± 0.13			
	300	1.19 ± 0.27	+4.08 ± 0.06	+11.2 ± 1.3	+23.8 ± 4.2
	305	1.78 ± 0.40			
	310	2.15 ± 0.49			
	315	2.66 ± 0.60			
Me (**5**)	270	0.28 ± 0.06			
	280	0.53 ± 0.12			
	290	0.77 ± 0.17	+3.68 ± 0.06	+12.6 ± 1.0	+30.0 ± 4.5
	295	1.15 ± 0.26			
	300	2.55 ± 0.58			
	305	3.70 ± 0.84			

plots for **3**, **4** and **5**. This only required that we allow for reduction in the concentration of the Mo(V) species in each case, since electronic spectra of **6** and **7** (Figures 5 and 6), the Mo(IV) and Mo(VI) disproportionation products from **3**, did not exhibit significant absorptions in the 500-nm region (ϵ_{515} = 80 L mol^{-1} cm^{-1} for **6**) and it seemed reasonable to assume that the spectra of **8** and **9** and of **10** and **11** would be similar to those of **6** and **7** respectively. As can be seen from Figure 2 the corrected plots showed excellent linearity and allowed the determination of the extinction coefficients for **3**, **4**, and **5** at 500 nm. These values were used in turn to correct the extinction coefficients for other absorption maxima in electronic spectra of **3**, **4**, and **5** (making appropriate allowances for the absorptions of Mo(VI) and M(IV)

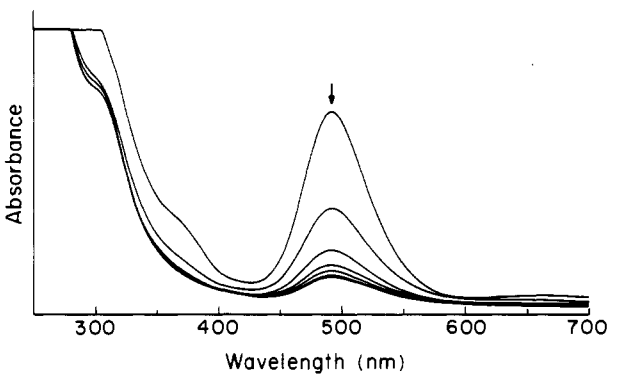

Figure 7. Photolysis of $[Mo_2O_3\{S_2P(OEt)_2\}_4]$ in CH_3CN.

Table VII. Electronic Spectral Data for Molybdenum Dialkyl Dithiophosphate Complexes in Toluene (Mo(V) Spectral Data Corrected for Dissociation)

compound	abs max, cm^{-1} × 10^{-3} (log ϵ)
$[Mo_2^{V}O_3\{S_2P(OEt)_2\}_4]$ (**3**)	14.9 (3.06), 20.0 (4.07), 27.0 (3.75)
$[Mo_2^{V}O_3\{S_2P(OPh)_2\}_4]$ (**4**)	15.2 (3.42), 20.0 (4.44), 27.0 (4.11)
$[Mo_2^{V}O_3\{S_2P(OMe)_2\}_4]$ (**5**)	14.7 (3.35), 20.0 (4.22), 27.0 (3.94)
$[Mo^{IV}O\{S_2P(OEt)_2\}_2]$ (**6**)	19.4 (1.90), 24.7 (sh)
$[Mo^{VI}O_2\{S_2P(OEt)_2\}_2]$ (**7**)	27.1 (3.43)

species in the UV). Table VII summarizes the electronic spectra of all three Mo(V) dimers after correction for the dissociation equilibria.

Dissociation constants for **3**, **4**, and **5** at each temperature were used to calculate ΔG for the dissociation reactions, and these were in turn used to calculate ΔH and ΔS for the reactions from plots of ΔG versus T. The equilibrium constants and derived thermodynamic parameters for **3**, **4**, and **5** are summarized in Table VI. The uncertainties were calculated on the assumption that the integrations had precisions of ±10%.

The observed dissociation constants for **3**, **4**, and **5** in toluene are in reasonable agreement with the value reported previously for **3** in 1,2-dichloroethane and the resulting positive deviations from Beer's law are similar to those reported for complexes such as $[Mo_2O_3(S_2CNEt_2)_4]$,[21] $[Mo_2O_3(S_2PPh_2)_4]$,[4] and $[Mo_2O_3(S_2CSR)_4]$ where R = Et, ^{i}Pr, ^{t}Bu, and CH_2Ph.[22] An extreme example of such a dissociative equilibrium in an $[Mo^{V}_2O_3]^{4+}$ complex has been reported in the case of $[Mo_2O_3(S_2CPh)_4]$, which disproportionates completely and irreversibly upon dissolution in 1,2-dichloroethane, as established by IR and UV–vis spectroscopies.[23]

The ΔH and ΔS values are similar in magnitude for disproportionation for all three $[Mo_2O_3\{S_2P(OR)_2\}_4]$ complexes. The modest positive values of ΔH (ca. +12 kcal mol^{-1}) establish that the disproportionation is entropically driven by the large positive values of ΔS of 23–30 eu arising from the dissociative nature of the reaction.

Wavelength-Dependent Photolysis of the Dithiophosphate Complexes 3, 4, and 5. Preliminary experiments readily established that the photochemical behavior of **3** differs markedly for that which we had previously established for the dithiocarbamate complexes **1** and **2**. Photolysis of **3** in CH_3CN, for example, caused an *irreversible* bleaching, as illustrated by the sequence in Figure 7 in which the electronic spectrum of a solution of **3** in CH_3CN was monitored at 5-min intervals during irradiation with unfiltered light from the Hg–Xe arclamp. There was a gradual decay of the 500-nm absorption into a weak band at 515 nm together with complete decay of the 370- and 670-nm

(21) Newton, W. E.; Corbin, J. L.; Bravard, D. C.; Searles, J. E.; McDonald, J. W. *Inorg. Chem.* **1974**, *13*, 1100.
(22) Hyde, J.; Venkatasubramanian, K.; Zubieta, J. *Inorg. Chem.*, **1978**, *17*, 414.
(23) Tatsumisago, M.; Matsubayashi, G.; Tanaka, T.; Nishigaki, S.; Nakatsu, K. *J. Chem. Soc., Dalton Trans.* **1982**, 121.

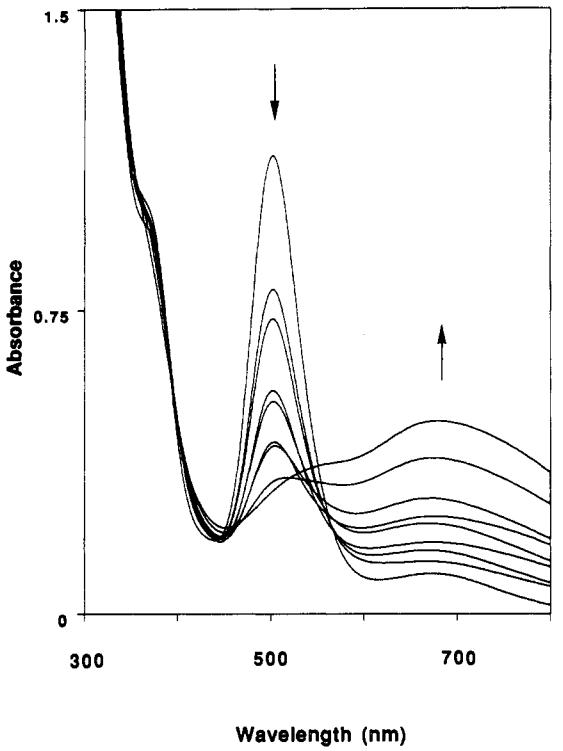

Figure 8. Photolysis of $[Mo_2O_3\{S_2P(OEt)_2\}_4]$ in toluene.

absorptions. The photolytic behavior of **3** differs only slightly in toluene as shown in Figure 8. There was again a gradual decay of the 370 and 500 nm bands, but new features now included a broad absorption at ca 680 nm.

In addition to its irreversibility the photochemical behavior of **3** differs from that of **1** and **2** in its wavelength dependence. Qualitative experiments using filters readily established that **3** was bleached upon irradiation by UV light (<400 nm) but was unaffected by visible light (>400 nm), even though the complex has an intense absorption at 500 nm. The photochemical behaviors of **4** and **5** were similar to that of **3**, indicating that irreversible wavelength-dependent photolysis is characteristic of dithiophosphate complexes of the $[Mo^V_2O_3]^{4+}$ unit.

The qualitative wavelength dependence observed for photolysis for **3**, **4**, and **5** was so marked (and so intriguing in the context of our interest in the potential applications of transition metal photochromics in optical memory systems as outlined in the Introduction), that we carried out a quantitative determination of the disappearance quantum yields for **3**, **4**, and **5** at a range of UV and visible wavelengths. The measurements were made as described in the Experimental Section using monochromatic light which had been passed through an appropriate interference filter. The disappearance quantum yields for the three complexes at various wavelengths are reported in Tables VIII–X.

The values are unremarkable with respect to their magnitude in the UV, with values ranging from a very modest 4.3×10^{-3} for **5** irradiated at 334 nm up to 1.8×10^{-2} for **4** irradiated at 310 nm. There is no significant wavelength dependence in the quantum yields as long as irradiation wavelengths between 310 and 365 nm are employed, with only marginal changes in Φ for any one compound with this range. What was intriguing, however, was that all three dimers were unaffected by irradiation at a wavelength of 510 nm, which almost directly coincides with their absorbance maxima at 500 nm. Under the conditions of the experiments this corresponds to an upper limit of 1×10^{-4} for the disappearance quantum yield for visible irradiation.

The implication of the data in Tables VIII–X is that all three complexes exhibit remarkable effective relative disappearance quantum yields in the UV and visible regions, with $\Phi_{310}:\Phi_{510}$ ratios of >150, >180, and >60 respectively for **3**, **4**, and **5**. Such values make little sense for a photochemical process involving a single molecule—there are well established examples of transition metal complexes which undergo wavelength dependent photochemistry,[24-26] but the effects are usually modest since the energy absorbed from a high energy photon is typically rapidly distributed over most of the states of a transition metal complex so that reactive states can be accessed from any state above the threshold value.[27]

Table VIII. Disappearance Quantum Yields for Loss of the 500-nm Band[a] of $[Mo_2^VO_3\{S_2P(OEt)_2\}_4]$ in Toluene at 30.0 °C[b]

λ, (nm)	concn, M × 10⁴	intens, einstein s⁻¹ × 10⁹	ΔA/t, s⁻¹ × 10⁴	quantum yield, Φ
310	5.73	12.4	8.15	0.017
			7.00	0.015
			6.75	0.014
				0.015 av
334	6.00	4.57	2.37	0.013
			2.38	0.013
			3.03	0.017
				0.014 av
365	7.72	12.4	8.53	0.017
			7.15	0.015
			7.49	0.015
				0.016 av

[a] ϵ_{500} = 11 800 L mol⁻¹ cm⁻¹. [b] No photolysis was observed ($\Phi < 1 \times 10^{-4}$) following irradiation at 510 nm.

Table IX. Disappearance Quantum Yields for Loss of the 500-nm Band[a] of $[Mo_2^VO_3\{S_2P(OPh)_2\}_4]$ in Toluene at 30.0 °C[b]

λ, nm	concn, M × 10⁴	intens, einstein s⁻¹ × 10⁹	ΔA/t, sec⁻¹ × 10⁴	quantum yield, Φ
310	3.66	3.79	6.28	0.018
			6.38	0.019
			6.14	0.018
				0.018 av
334	3.66	0.95	0.98	0.011
			0.90	0.010
			1.03	0.012
				0.011 av

[a] ϵ_{500} = 27 200 L mol⁻¹ cm⁻¹. [b] No photolysis was observed ($\Phi < 1 \times 10^{-4}$) following irradiation at 510 nm.

Table X. Disappearance Quantum Yields for Loss of the 500-nm Band[a] of $[Mo_2^VO_3\{S_2P(OMe)_2\}_4]$ in Toluene at 30.0 °C[b]

λ, nm	concn, M × 10⁴	intens, einstein s⁻¹ × 10⁹	ΔA/t, s⁻¹ × 10⁴	quantum yield, Φ
310	3.08	11.7	6.74	0.0066
			6.09	0.0059
			6.29	0.0061
				0.0062 av
334	3.08	3.73	1.24	0.0037
			1.57	0.0047
			1.43	0.0043
				0.0043 av

[a] ϵ_{500} = 16 600 L mol⁻¹ cm⁻¹. [b] No photolysis was observed ($\Phi < 1 \times 10^{-4}$) following irradiation at 510 nm.

(24) For a discussion, see: Bock, C. R.; Koerner von Gustorf, E. A. *Adv. Photochem.* **1977**, *10*, 221.
(25) For early examples, see: (a) Wrighton, M.; Hammond, G. S.; Gray, H. B. *J. Am. Chem. Soc.* **1971**, *93*, 4336. (b) Wrighton, M.; Hammond, G. S.; Gray, H. B. *Mol. Photochem.* **1973**, *5*, 179. (c) Wrighton, M. *Inorg. Chem.* **1974**, *13*, 905. (d) Wrighton, M. S.; Morse, D. L.; Gray, H. B.; Ottsen, D. K. *J. Am. Chem. Soc.* **1976**, *98*, 1111.
(26) For recent leading references see: (a) Johnson, C. E.; Trogler, W. C. *J. Am. Chem. Soc.* **1981**, *103*, 6352. (b) Chang, I. J.; Nocera, D. G. *J. Am. Chem. Soc.* **1987**, *109*, 4901. (c) van Dijk, H. K.; Stufkens, D. J.; Oskan, A. *J. Am. Chem. Soc.*, **1989**, *111*, 541.

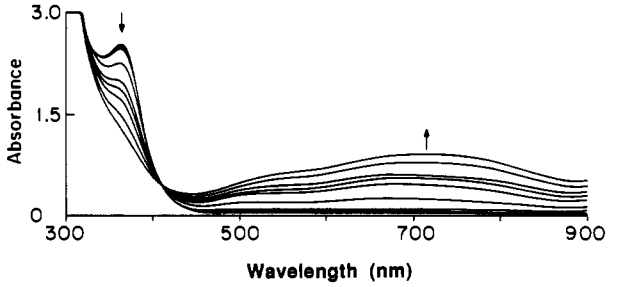

Figure 9. Photolysis of $[MoO_2\{S_2P(OEt)_2\}_2]$ in toluene.

The only reasonable interpretation of the observed wavelength dependence for the photolysis of **3** is that the Mo(V) dimer is not itself the photoactive species, but that it is destroyed through photolysis of one or both of the Mo(IV) and Mo(VI) disproportionation products. Since it is only the Mo(V) dimer which absorbs significantly in the 500 nm region, as can be seen by inspection of the electronic spectra in Figures 2a, 5, and 6, there would then be no net photolysis of **3** following irradiation in the 500-nm region.

Photosensitivity of the Mo(IV) and Mo(VI) Complexes $[MoO\{S_2P(OEt)_2\}_2]$ (6) and $[MoO_2\{S_2P(OEt)_2\}_2]$ (7). The hypothesis that the Mo(IV) and/or Mo(VI) complexes **6** and **7** were the photoactive species in solutions of **3** was readily tested since the Mo(IV) disproportionation product **6** is a known complex and we had succeeded in synthesizing the Mo(VI) disproportionation product by oxidation of **3** as described above.

Preliminary experiments readily established that it is **7** rather than **6** which is photoactive. Solution of **6** could be irradiated with a Pyrex-filtered 200-W arc lamp for up to 1 h without significant change in ^{31}P NMR spectra, but **7** proved to be markedly photosensitive at 365 nm (200-W arc lamp, 365-nm interference filter). Irradiation in this region (Figure 9) caused the 369-nm band in the electronic spectra to be replaced by a very broad band at ca. 700 nm with a poorly defined shoulder at ca. 585 nm. This corresponds to a change in the color of the solution from pale yellow to a blue, a color change similar to that reported for the thermal decomposition of thioxanthate dimers[22] and reminiscent of mixed-valent polymolybdate anions ("molybdenum blues").[28] These anions contain both Mo(V) and Mo(VI) centers, and could arise in this system from the photolytic loss of a diethyl dithiophosphate ligand or ligands from **7**. Peterson and Richman have reported[29] that irradiation in 1,2-dichloroethane at 23 °C into the 380-nm band of $[MoO_2(S_2CNEt_2)_2]$ (a Mo(VI)–dioxo complex related to **7**) results in loss of a dithiocarbamate radical with a quantum yield of 2.07×10^{-2}. A subsequent dark radical chain reaction leads ultimately to formation of $(S_2CNEt_2)_2$ and a gray precipitate formulated as "oxides of molybdenum" on the basis of IR data and X-ray powder diffraction data. Similar photolytic ligand loss has been observed for molybdenum(VI) thioxanthate complexes as established by IR spectroscopy and cyclic voltammetry.[22] It is possible that **7** also undergoes a similar photolytic ligand loss to give organic products and molybdenum oxides, but ^{31}P NMR spectra of samples irradiated in an NMR tube have established the formation of a complex mixture of ^{31}P containing products, and we have not determined the nature of the photolysis products formed from **7**.

(27) (a) Adamson, A. W.; Fleischauer, P. D. *Concepts of Inorganic Photochemistry*; Krieger: Malabar, FL, 1984. (b) Ferraudi, G. J. *Elements of Inorganic Photochemistry*; Wiley: New York, 1988.
(28) Cotton, F. A.; Wilkinson, G. *Advanced Inorganic Chemistry*; 5th ed.; Wiley: New York; 1988; p 818.
(29) Peterson, M. W.; Richman, R. M. *Inorg. Chem.* **1982**, *21*, 2609.

Table XI. Disappearance Quantum Yields for Loss of the 369-nm Band[a] of $[Mo^{VI}O_2\{S_2P(OEt)_2\}_2]$ in Toluene at 30.0 °C

λ, nm	concn, $M \times 10^4$	intens, einsten $s^{-1} \times 10^9$	$\Delta A/t$, $s^{-1} \times 10^4$	quantum yield, Φ
310	8.74	2.56	2.66	0.12
			2.65	0.13
			2.62	0.12
				0.12 av
334	8.38	4.45	4.07	0.10
			3.61	0.093
			3.73	0.096
				0.098 av
365	8.38	13.9	13.3	0.11
			12.8	0.11
			12.3	0.10
				0.11 av

[a] $\epsilon_{369} = 2630$ L mol^{-1} cm^{-1}.

Disappearance quantum yields at 369 nm for irradiation of **7** in toluene were determined as described in the Experimental Section. The results are summarized in Table XI and it is immediately apparent that photolysis of **7** is much more efficient than photolysis of **3**, with a disappearance quantum yield about an order of magnitude higher for **7** than for **3** following irradiation in the UV region. It is, of course, necessary that photolysis of **7** be more efficient than photolysis of **3** if **7** is to be the only major photoactive species in solutions of **3**, since internal screening will reduce the effective intensity of the light which acts on **7** and the concentrations of **7** will be only a fraction of that of the added **3**. To put it another way, it is because only a small mole fraction of the added **3** is present as **7**, and because this **7** is further subject to photochemically unproductive internal screening by the **6** and **3** present, that the effective disappearance quantum yield for **3** (and, by analogy, the similar quantum yields for **4** and **5**) are so low.

Conclusions

Quantification by ^{31}P NMR has confirmed that deviations from Beer's law in solutions of **3**, **4** and **5** are due to dissociative equilibria between the d^1–d^1 oxo-bridged dimers and their d^0 and d^2 disproportionation products of the type $[MoO_2\{S_2P(OR)_2\}_2]$ and $[MoO\{S_2P(OR)_2\}_2]$. The thermal accessibility of the d^0 monomers $[MoO_2\{S_2P(OR)_2\}_2]$ is central to the observed photochemistry of the d^1–d^1 dimers, which undergo irreversible photolysis with effective disappearance quantum yields of 10^{-3}–10^{-2} when irradiated below 400 nm but which are stable to irradiation into their major visible absorptions at 500 nm. We propose that it is the d^0 monomers which are photosensitive and *not* the d^1–d^1 dimers, as confirmed in the $S_2P(OEt)_2$ system by the independent determination that $[MoO_2\{S_2P(OEt)_2\}_2]$ (**7**) has a disappearance quantum yield of ca. 0.1 for irradiation at 310 nm. This would provide a satisfactory explanation for the marked wavelength dependence observed for photolysis of **3**, **4**, and **5** and raises the intriguing question of how generally thermal equilibria can be used to tune the wavelength dependence of the photochemical properties of transition metal complexes.

Acknowledgment. This work was supported in part by the Office of Naval Research. We thank Dr. Ceci Philbin for guidance in the measurement of the quantum yields, and Professor Greg Geoffroy for the gift of a sample of Aberchrome 540.

Supplementary Material Available: Anisotropic displacement coefficients for **5** (Table IS) and H-atom coordinates and isotropic displacement coefficients for **5** (Table IIS) (1 page). Ordering information is given on any current masthead page.